Hydrol. Earth Syst. Sci. Discuss., https://doi.org/10.5194/hess-2018-18
Manuscript under review for journal Hydrol. Earth Syst. Sci.
Discussion started: 31 January 2018

Hydrology and Earth System Sciences
Discussions

Multi-source data assimilation for physically-based hydrological modeling of an experimental hillslope

Anna Botto[1], Enrica Belluco[1], and Matteo Camporese[1]

[1]Department of Civil, Environmental and Architectural Engineering, University of Padova, Italy

Correspondence to: Anna Botto (anna.botto@unipd.it)

Abstract.

Data assimilation has been recently the focus of much attention for integrated surface-subsurface hydrological models, whereby joint assimilation of water table, soil moisture, and river discharge measurements with the ensemble Kalman filter (EnKF) have been extensively applied. Although the EnKF has been specifically developed to deal with nonlinear models, integrated hydrological models based on the Richards equation still represent a challenge, due to strong nonlinearities that may significantly affect the filter performance. Thus, more studies are needed to investigate the capabilities of the EnKF to correct the system state and identify parameters in cases where the unsaturated zone dynamics are dominant, as well as to quantify possible tradeoffs associated with assimilation of multi-source data. Here, the model CATHY (CATchment HYdrology) is applied to reproduce the hydrological dynamics observed in an experimental two-layered hillslope, equipped with tensiometers, water content reflectometer probes, and tipping bucket flow gages to monitor the hillslope response to a series of artificial rainfall events. Pressure head, soil moisture, and subsurface outflow are assimilated with the EnKF in a number of scenarios and the challenges and issues arising from the assimilation of multi-source data in this real-world test case are discussed. Our results demonstrate that the EnKF is able to effectively correct states and parameters even in a real application characterized by strong nonlinearities. However, multi-source data assimilation may lead to significant tradeoffs: the assimilation of additional variables can lead to degradation of model predictions for other variables that were otherwise well reproduced. Furthermore, we show that integrated observations such as outflow discharge cannot compensate for the lack of well-distributed data in heterogeneous hillslopes.

1 Introduction

Data assimilation, i.e., the process in which observations of a system are merged in a consistent manner with numerical model predictions (e.g., Troch et al., 2003; Moradkhani, 2008), has become increasingly popular in hydrological modeling over the last few decades (Montzka et al., 2012). Among the various techniques available, the ensemble Kalman filter (EnKF) (Evensen, 2003, 2009b) is probably the most widespread, thanks to its ease of implementation, capability to handle nonlinear models and potential to be used as a sequential inverse modeling tool when parameters are included in the update step. Applications in hydrology include studies in different disciplines, such as groundwater hydrology (e.g., Chen and Zhang, 2006; Hendricks Franssen and Kinzelbach, 2008; Bailey and Baù, 2010; Li et al., 2012; Zovi et al., 2017), rainfall-runoff modeling

(e.g., Moradkhani et al., 2005; Vrugt et al., 2006; Weerts and El Serafy, 2006; Clark et al., 2008; Xie and Zhang, 2010; Han and Li, 2008), and land surface modeling at multiple scales (e.g., Reichle et al., 2002a, b; Crow and Wood, 2003; Francois et al., 2003; Pan and Wood, 2006; De Lannoy et al., 2007; Cammalleri and Ciraolo, 2012; Flores et al., 2012; Hain et al., 2012).

As a consequence of such popularity, the EnKF is more and more applied also with integrated surface-subsurface hydrological models (IHSSMs), whereby multiple terrestrial compartments (e.g., snow cover, surface water, groundwater) are solved simultaneously, in an attempt to tackle environmental problems in a holistic approach (Maxwell et al., 2014; Kollet et al., 2017). For instance, Camporese et al. (2009a) and Camporese et al. (2009b) combined the CATHY model and the EnKF to assimilate pressure head, soil moisture, and streamflow data, finding that the assimilation of pressure head and soil moisture is beneficial to subsurface states and river discharge, but the assimilation of river discharge alone does not improve the prediction of subsurface states. Similar conclusions were drawn by Pasetto et al. (2012), who compared the EnKF with a modified particle filter to assimilate discharge and pressure head, again with the CATHY model. More recently, Pasetto et al. (2015) used the EnKF and CATHY to investigate the impact of possible sensor failure on the observability of flow dynamics and estimation of the model parameters characterizing the soil properties of an artificial hillslope. Ridler et al. (2014) assimilated soil moisture remote sensing products in the MIKE SHE model and found that surface soil moisture has correction capabilities limited to the first 25 cm of soil. With the same model, Rasmussen et al. (2015a), Rasmussen et al. (2015b), Zhang et al. (2015), and Zhang et al. (2016) investigated in detail issues related to uncertainty quantification and biased observations, as well the impacts of update localization and ensemble size on the multivariate assimilation of groundwater head and river discharge at the catchment scale. Kurtz et al. (2016) first presented a data assimilation framework for the land surface-subsurface part of the Terrestrial System Modelling Platform (TerrSysMP), followed by Baatz et al. (2017), who assimilated distributed river discharge data into the TerrSysMP to estimate the spatially distributed Manning's roughness coefficient, and Zhang et al. (2018), who tested and compared five data assimilation methodologies for assimilating groundwater level data via the EnKF to improve root zone soil moisture estimation. Within yet another modeling framework, Tang et al. (2017) used the EnKF in conjunction with HydroGeoSphere to study the influence of heterogeneous riverbeds on river-aquifer exchange fluxes.

In spite of such a strong interest, several issues related to the use of EnKF for state and parameter estimation in integrated hydrological modeling remain unresolved. The subsurface component of many IHSSMs is based on the solution of the Richards equation in one or three dimensions and although recent studies in synthetic experiments (Erdal et al., 2014; Brandhorst et al., 2017) have shown that the EnKF has great potential for the estimation of soil hydraulic parameters in the unsaturated zone, it is still unclear whether the method is able to cope with nonlinearities and parameter estimation in real test cases, where multiple uncertainties on initial and boundary conditions make the problem much more challenging (e.g., Visser et al., 2006; De Lannoy et al., 2007; Monsivais-Huertero et al., 2010; Shi et al., 2015). Also, as more sources of data become available at cheaper costs, it is increasingly difficult to assess which data types are the most suitable or effective to assimilate and in general to assess possible tradeoffs related to multivariate data assimilation.

Within this context, the main goals of the present study are: i) to assess whether the EnKF in combination with a Richards equation-based hydrological model is able to effectively improve states and parameters in a real-world test case characterized by dominant unsaturated dynamics and ii) to quantify the tradeoffs associated to multi-source data assimilation. To pursue

Hydrol. Earth Syst. Sci. Discuss., https://doi.org/10.5194/hess-2018-18
Manuscript under review for journal Hydrol. Earth Syst. Sci.
Discussion started: 31 January 2018

Hydrology and Earth System Sciences
Discussions

these goals, the EnKF is used in combination with the CATHY (CATtchment HYdrology) model (Camporese et al., 2010) to assimilate real observations of pressure head, soil moisture and subsurface outflow collected during a controlled experiment carried out in an artificial hillslope. The experiment is characterized by strong nonlinearities, due to the dominant unsaturated dynamics, but the strictly controlled conditions, as opposed to field studies, allow us to minimize the effects of initial and boundary conditions uncertainty on the problem at hand. The behavior and performance of the EnKF-based assimilation framework in terms of its ability to retrieve the correct hillslope response are evaluated in a number of data assimilation scenarios, characterized by different combinations of assimilated and updated variables.

2 The hillslope experiment

The artificial hillslope is placed inside a concrete structure of lenght 6 m, width 2 m, and height varying linearly from 3.5 m to 0.5 m, corresponding to a slope of 32 degrees. A total of fifty apertures, which can be kept closed with screw cups when needed, allow the positioning of various monitoring sensors in properly chosen positions on each lateral wall of the structure. The hillslope toe is made with a hollow-brick porous wall, in order to allow subsurface water to drain. The soil was placed inside the structure to mimic a two-layered hillslope. A uniform 60 cm-thick silty fine sand was deployed on top of a relatively impermeable basement made of sandy clay soil. More details on the soil properties can be found in Lora et al. (2016) and Schenato et al. (2017). In the following, we will refer to the two soil types simply as sand and clay.

Six tensiometers and six water content reflectometer (WCR) probes are used to measure pressure head and water content in the top soil layer. All the sensors are located in an intermediate position of the hillslope, as shown in Figure 1, which reports a plan view and longitudinal cross-section along with the six positions where each tensiometer has been installed in front of the corresponding WCR. Two tipping-bucket flow gages are placed at the toe of the hillslope to measure surface runoff and subsurface outflow, while the rain is generated by a rainfall simulator that can produce relatively uniform rainfall intensities varying from 50 to 150 mm/h (Lora et al., 2016).

A Campbell Scientific (CR 1000) data logger has been used to collect and record all the data with a frequency of 0.5 Hz during a 12-day experiment, which has been carried out by generating rainfall events of different duration alternated with recession periods. Before the experiment, two preliminary tests have been performed to check the intensity and the uniformity of the rainfall rate. The coefficient of uniformity of the preliminary tests resulted equal to 72%, for a mean rate of 58.8 mm/h. Figure 2 reports all the data collected during the experiment. Note that the tensiometers P1 and P4 were affected by malfunctioning, therefore their data are not reported and will not be used in the data assimilation simulations.

3 Numerical methods

3.1 The CATHY model

The CATHY (CATchment HYdrology) model (Camporese et al., 2010) is a physics-based hydrological model capable of simulating integrated subsurface, overland and channel water flow. The model combines a Richards equation solver for the

Hydrol. Earth Syst. Sci. Discuss., https://doi.org/10.5194/hess-2018-18
Manuscript under review for journal Hydrol. Earth Syst. Sci.
Discussion started: 31 January 2018

three-dimensional flow in variably saturated porous media with a surface water flow module for the solution of the one-dimensional diffusion wave approximation of the De saint Venant equation. In this study, however, there is no surface runoff. Therefore, only subsurface flow is considered, according to the following form of Richards equation:

$$S_w S_s \frac{\partial \psi}{\partial t} + \phi \frac{\partial S_w}{\partial t} = \nabla [K_s K_r \nabla \psi + \eta_z] + q_s. \tag{1}$$

In equation (1), $S_w = \theta/\phi$ is water saturation, θ and ϕ being the volumetric soil water content and porosity $[/]$, respectively, S_s is the specific storage coefficient $[L^{-1}]$, ψ is the pressure head $[L]$, t is time $[T]$, ∇ is the gradient operator, K_s is the saturated hydraulic conductivity tensor $[L/T]$, K_r is the relative hydraulic conductivity function $[/]$, $\eta_z = (0,0,1)^T$ is the vertical direction vector, z is the vertical coordinate directed upward $[L]$, and q_s represents distributed source or sink terms $[L^3/L^3T]$.

The unsaturated hydraulic properties are taken into account by means of the van Genuchten (1980) functions $S_w(\psi)$ and $K_r(\psi)$:

$$S_w = S_{wr} + \frac{1 - S_{wr}}{[1 + (\alpha|\psi|)^n]^m}, \tag{2}$$

$$K_r = \left(\frac{S_w - S_{wr}}{1 - S_{wr}} \right)^{0.5} \left\{ 1 - \left[1 - \left(\frac{S_w - S_{wr}}{1 - S_{wr}} \right)^{\frac{1}{m}} \right]^m \right\}^2, \tag{3}$$

where $S_{wr} = \theta_r/\phi$ is the residual water saturation, with θ_r the residual water content, α is an empirical constant $[L^{-1}]$ related to the inverse of the air entry suction, while the dimensionless shape parameters n and m are linked by the expression $m = 1 - 1/n$.

Equation (1) is solved by means of Galerkin finite elements with tetrahedral elements and linear basis functions in space and weighted finite differences for integration in time (Camporese et al., 2010).

3.2 The ensemble Kalman filter

The ensemble Kalman filter (Evensen, 2003, 2009a, b) is a sequential data assimilation scheme, in which states (and parameters) are sequentially updated based on a Monte Carlo approximation of the covariance matrices needed in the standard Kalman filter. The process is Markovian of the first order and the implementation of the EnKF does not require the linearization of the model, making it particularly suitable to handle non-linear problems.

In this paper the EnKF is implemented according to the numerical formulation proposed by Sakov et al. (2010). Let $\mathbf{X}$ be an ensemble matrix of M rows and N columns, where N is the number of realizations and M is the state dimension, i.e., the number of nodes in the finite element grid, augmented by the number of parameters that are subject to update. The main idea behind this type of implementation is that the matrix $\mathbf{X}$ can be defined as the sum, $\mathbf{x} + \mathbf{A}$, of the ensemble average, $\mathbf{x}$,

$$\mathbf{x} = \frac{1}{N} \mathbf{X} \mathbf{1}, \tag{4}$$

and the matrix of ensemble anomalies, $\mathbf{A}$,

$$\mathbf{A} = \mathbf{X}(\mathbf{I} - \frac{1}{N} \mathbf{1}\mathbf{1}^T), \tag{5}$$

Hydrol. Earth Syst. Sci. Discuss., https://doi.org/10.5194/hess-2018-18
Manuscript under review for journal Hydrol. Earth Syst. Sci.
Discussion started: 31 January 2018

where $\mathbf{1}$ and $\mathbf{I}$ are a vector with all elements equal to one and the identity matrix, respectively. As usual, superscript T denotes matrix transposition.

Whenever observed data are available, the EnKF can compute the updated matrix $\mathbf{X}^u$ as the sum of the updated ensemble mean, $\mathbf{x}^u$, and the updated anomalies, $\mathbf{A}^u$,

$$\mathbf{X}^u = \mathbf{x}^u + \mathbf{A}^u. \tag{6}$$

In the following, the lack of a superscript u denotes that the matrix or vector is computed at the forecast stage, i.e., at the previous model time step.

The updated mean can be calculated as

$$\mathbf{x}^u = \mathbf{x} + \boldsymbol{\beta}\mathbf{A}\mathbf{G}\mathbf{s}, \tag{7}$$

where $\boldsymbol{\beta}$ is a diagonal matrix of dampening factors (Hendricks Franssen and Kinzelbach, 2008), whose elements vary from 0 to 1, $\mathbf{s}$ is the scaled innovation vector

$$\mathbf{s} = \mathbf{R}^{-1/2}(\mathbf{D} - \mathbf{H}\mathbf{x})/\sqrt{N-1}, \tag{8}$$

which depends on the measurement error covariance matrix, $\mathbf{R}$, and on the difference between the measurements, $\mathbf{D}$, and the ensemble mean of the simulated observations, $\mathbf{H}\mathbf{x}$.

The matrix $\mathbf{G}$ is defined as

$$\mathbf{G} = \mathbf{M}\mathbf{S}^T, \tag{9}$$

where $\mathbf{S}$ is the matrix of scaled ensemble innovation anomalies

$$\mathbf{S} = \mathbf{R}^{-1/2}\mathbf{H}\mathbf{A}/\sqrt{N-1}, \tag{10}$$

$\mathbf{H}\mathbf{A}$ being the simulated measurement anomalies

$$\mathbf{H}\mathbf{A} = \mathbf{H}\mathbf{X}(\mathbf{I} - \frac{1}{N}\mathbf{1}\mathbf{1}^T), \tag{11}$$

and $\mathbf{M}$ being defined as

$$\mathbf{M} = (\mathbf{I} + \mathbf{S}^T\mathbf{S})^{-1}. \tag{12}$$

The updated anomalies, $\mathbf{A}^u$, are computed as

$$\mathbf{A}^u = \mathbf{A} + \boldsymbol{\beta}\mathbf{A}(\mathbf{M}^{1/2} - \mathbf{I}). \tag{13}$$

When updating the states only, the elements of $\mathbf{X}$ are the pressure heads at each node of the finite element grid, while the state augmentation technique is used when updating also the parameters. In this latter case, the desired parameters (e.g., hydraulic conductivity, parameters of the retention curves), transformed as described in section 4.2, are added to $\mathbf{X}$ and updated based on their correlation with the system states (e.g., Erdal et al., 2015).

Hydrol. Earth Syst. Sci. Discuss., https://doi.org/10.5194/hess-2018-18
Manuscript under review for journal Hydrol. Earth Syst. Sci.
Discussion started: 31 January 2018

4 Model and data assimilation setup

4.1 CATHY setup

The artificial hillslope is discretized with a surface triangular grid resulting from the subdivision of square cells of 10 cm side. The triangular grid is then replicated vertically for a total of 25 layers to generate the three-dimensional tetrahedral mesh (Figure 3). Fifteen layers are used to represent the top sand, while 10 layers discretize the clay. No flow boundary conditions are assumed at each boundary, except for the subsurface outflow section, where seepage face boundary conditions are used, and the surface, where rainfall and evaporation rates are imposed. Finally, the soil hydraulic parameters are assigned as reported in Table 1. The values of saturated hydraulic conductivity and van Genuchten retention parameters are perturbed to generate the ensemble of realizations as described in the following section, while soil porosities and specific storages are considered deterministic, as the former were well characterized with laboratory tests, while the CATHY model is usually not very sensitive to the latter.

4.2 EnKF setup

In order to generate the ensemble of realizations needed for the application of the EnKF, we perturb the atmospheric forcing (i.e., rainfall and evaporation rates), soil properties, and initial conditions. Table 1 reports a summary of the perturbed variables, along with their nominal mean values as well as the nature and statistics of the perturbations. The ensemble of time-variable atmospheric forcing rates was generated with a sequence of multiplicative perturbations, $\mathbf{q_k}$, correlated in time as in Evensen (2003),

$$\mathbf{q}_k = \gamma \mathbf{q}_{k-1} + \sqrt{1-\gamma^2}\mathbf{w}_{k-1}, \tag{14}$$

where the subscript k is the time index, $\mathbf{w_k}$ is a sequence of white noise drawn from the standard normal distribution, and the coefficient γ is computed as

$$\gamma = 1 - \frac{\Delta t}{\tau}, \tag{15}$$

Δt being the assimilation interval and τ the specified time decorrelation length, here set equal to 108,000 s, i.e., 30 h.

The initial conditions consist of a uniform value of pressure head, ψ_0, whose nominal ensemble mean is -0.67 m, corresponding to a fully unsaturated soil. The ensemble of ψ_0 values is generated by additive perturbations normally distributed with mean equal to 0 and standard deviation equal to 0.2 m.

Perturbed soil parameters, for both sand and clay, include the saturated hydraulic conductivity as well as the parameters of the van Genuchten retention curves. Table 1 reports the nominal mean values of K_s, based on soil samples analyzed in the laboratory, as well as the parameters used for generating their ensembles. The saturated hydraulic conductivities of sand and clay are perturbed independently from each other with multiplicative perturbations sampled from a lognormal distribution.

The parameters of the van Genuchten retention curves α, n, and θ_r are perturbed taking into account their mutual correlation according to Carsel and Parrish (1988), who described their statistics and transformed them into normally distributed variables

Hydrol. Earth Syst. Sci. Discuss., https://doi.org/10.5194/hess-2018-18
Manuscript under review for journal Hydrol. Earth Syst. Sci.
Discussion started: 31 January 2018

Hydrology and Earth System Sciences
Open Access
Discussions

via the Johnson system (Johnson, 1970; Bertino et al., 2003). Three main transformation functions are used, i.e, the lognormal (LN), log-ratio (SB), and hyperbolic (SU):

$$LN: Y = ln(V) \tag{16}$$

$$SB: Y = ln[(V - A)/(B - V)] = ln(U) \tag{17}$$

$$SU: Y = sinh^{-1}(U), \tag{18}$$

where V denotes the parameter before transformation, bounded within the range $[A\ B]$, and Y denotes the transformed parameter with normal distribution. In this work, the prior statistics of the van Genuchten parameters are taken from the soil types "sandy loam" and "silt loam" in Carsel and Parrish (1988), assumed as valid representations of our sand and clay, respectively. The ensemble of transformed parameters is generated by

$$\mathbf{y} = \mathbf{u} + \mathbf{T}^{\mathbf{T}}\mathbf{z}, \tag{19}$$

where $\mathbf{y}$ is the vector containing transformed α, n, and θ_r, $\mathbf{u}$ contains the transformed variable means, $\mathbf{T}$ is the factored covariance matrix (see Table 2), and $\mathbf{z}$ is a vector of normal deviates with mean equal to 0 and standard deviation σ_{VG}. The transformed variables can be included in the matrix $\mathbf{X}$ when updating the parameters, and can then be back-transformed in order to obtain the updated values of the soil retention parameters.

The EnKF algorithm implemented here is actually an ensemble transform Kalman filter (Bishop et al., 2001) that does not require the perturbation of observations. However, the measurement error covariance matrix, $\mathbf{R}$, is assumed to be known a priori. In this work, $\mathbf{R}$ was estimated directly from the measurements, taking advantage of the high time resolution of the collected data. Pressure head and water content data were collected every 2 s and averaged every 10 min over a 40 s window to obtain the observations to assimilate. Over the same time window, the data were linearly detrended and the residuals used to calculate the correlation coefficients between all pairs of observations. The final covariance matrices were then assembled multiplying the correlation coefficients by the relevant standard deviations, assumed as 0.05 m and 0.025 for pressure head and water content, respectively. The subsurface outflow measurements are assumed independent from the pressure head and water content data, with a standard deviation equal to 8% of the measured discharge. When assimilating multiple variables, proper normalization of the measurement error covariance matrices, anomalies of the simulated data, and innovation vectors were performed, using values of 0.6 m, 0.58, and 4.17×10^{-5} m^3/s for pressure head, water content, and subsurface outflow, respectively.

4.3 Data assimilation scenarios

A total of 17 data assimilation scenarios have been simulated, whereby we varied the assimilation interval, the assimilated variables, the updated variables, and the uncertainty on the van Genuchten retention parameters. Table 3 reports a summary of the main characteristics for each scenario. Assimilated variables may include water content only or with subsurface outflow, pressure head only or with subsurface outflow, and all three variables together. As regards the updated variables, three cases have been analyzed: update of the state variables only; update of the state variables and saturated hydraulic conductivities for

Hydrol. Earth Syst. Sci. Discuss., https://doi.org/10.5194/hess-2018-18
Manuscript under review for journal Hydrol. Earth Syst. Sci.
Discussion started: 31 January 2018

both sand and clay; update of the state variables, hydraulic conductivities and van Genuchten parameters, for both sand and clay. In all the data assimilation scenarios, observations were assimilated only during the first five days of simulation, leaving the final seven days as a validation period, during which the ensemble was let to evolve freely. For comparison, two open loop simulations, i.e., without data assimilation, have also been carried out (Table 3).

The performance of the simulations has been evaluated by means of the root mean square error ($RMSE$), computed for the different variables, i.e., pressure head, water content, and subsurface outflow. The root mean square error is calculated as

$$RMSE(t) = \frac{1}{N_o}\sum_{j=1}^{N_o}\sqrt{\frac{1}{N}\sum_{i=1}^{N}\Big(S_{i,j}(t) - O_j(t)\Big)^2}, \tag{20}$$

where N_o is the number of observations available (six, four, and one for water content, pressure head, and subsurface outflow, respectively), $S_{i,j}$ refers to the simulated results of the ith realization of the ensemble at the location of the jth observation and O_j is the corresponding experimental value. To obtain a meaningful comparison between the errors of different variables, we also compute the time-averaged normalized root mean square error, $NRMSE$,

$$NRMSE = \frac{1}{N_T}\sum_{k=1}^{N_T}\frac{RMSE_k}{NF}, \tag{21}$$

where N_T is the number of time steps, k is the time index, and NF is a normalization factor equal to 0.58, 0.60 m, and 4.17×10^{-5} m^3/s (i.e., 2.5 l/min) for the water content, pressure head, and subsurface discharge, respectively. The $NRMSE$ is computed separately for each variable and for the assimilation ($N_T = 120$) and validation ($N_T = 167$) periods, but also as a global index of performance averaged over all the variables and the two periods.

5 Results and discussion

5.1 Preliminary simulations

A preliminary sensitivity analysis over a number of EnKF parameters has been performed, in order to select a final and satisfactory setup for the subsequent data assimilation scenarios. First, simulations with N equal to 32, 128 and 256 have been performed and it has been found that an ensemble size of 128 ensures a good tradeoff between performance and computational effort.

Then, several dampening factor values (β in equations (7) and (13)) have been tried, including combinations of different values for the update of system state and parameters. Based on this analysis, a value of 1 has been chosen for the update of the system state, whereas a dampening factor equal to 0.5 has been selected for the update of the soil hydraulic parameters (K_s, α, n, and θ_r, for both sand and clay). This choice of the dampening factors is consistent with previous studies (Brandhorst et al., 2017) and prevents abrupt changes of the retention curve parameters that could lead to difficulties in model convergence and hence loss of realizations.

According to these preliminary analyses, all scenarios reported in Table 3 have been simulated with an ensemble size of 128 and dampening factors of 1 and 0.5 for system state and parameters, respectively.

Hydrol. Earth Syst. Sci. Discuss., https://doi.org/10.5194/hess-2018-18
Manuscript under review for journal Hydrol. Earth Syst. Sci.
Discussion started: 31 January 2018

5.2 Overall EnKF performance

Table 4 and Figure 4 summarize the performance of the EnKF in all the data assimilation scenarios, expressed in terms of $NRMSE$ for the three measured variables (water content, WC, pressure head, PH, and subsurface outflow, Q), and averaged separately over the assimilation and validation windows. A comparison between scenarios 1-5 and 8-12 in Table 4, characterized by the same assimilated and updated variables but different assimilation intervals, show that assimilating more frequently does not always result in significant improvements of model predictions. The variable that benefits more from more frequent updates is subsurface outflow, especially in the scenarios where Q is assimilated (e.g., compare scenarios 3-5 with 10-12).

Figure 4 highlights that most of the data assimilation scenarios result in an improvement of model predictions for pressure head and subsurface outflow, compared to the open loop simulations (data pairs below the 45-degree reference line). However, there are some scenarios in which the filter performance in predicting water content is actually worse than in the open loop. From a close inspection of the values in Table 4, it is possible to identify such scenarios as those where pressure head is assimilated, alone or in conjunction with water content and subsurface outflow. This is probably due to a combination of two factors: i) only four out of six tensiometers are available for assimilation, compared to the six WCR probes available for water content, and ii) the pressure head measurements are characterized by relatively poor quality. This can be appreciated from the pressure head data shown in Figure 2, where diurnal disturbances caused by temperature fluctuations (Warrick et al., 1998) are apparent.

5.3 Parameter estimation capabilities

To assess the capabilities and benefits of parameter estimation with the EnKF, it is useful to compare scenarios with the same assimilated variables but different updated variables. Figures 5a, 5c, and 5e show the ratios between $RMSE$ in data assimilation scenarios S6, S8, S13 and the corresponding open loop values for water content, pressure head, and subsurface outflow, respectively. In these three scenarios, water content alone is assimilated, but the updated variables are system state only in S6, system state and saturated hydraulic conductivity in S8, and system state plus K_s and van Genuchten parameters α, n, and θ_r in S13. Figure 5a highlights that progressively updating more parameters brings significant improvements in water content prediction over the validation period, with reductions of the $NRMSE$ with respect to the open loop of almost 20% when updating K_s only and 60% when updating also the retention curve parameters. Moreover, updating parameters improves significantly pressure head predictions in validation and subsurface outflow in both assimilation and validation, as shown in Figures 5c and 5e.

The effect of parameter updating on model predictions for scenarios S6, S8, and S13 can be visualized in Figure 6, which shows ensemble means and 90% confidence bands of simulated water content, pressure head, and subsurface outflow in comparison with the experimental data and the corresponding open loop values. In scenario S6, without parameter update, model predictions during the validation tend to converge again to the open loop simulations both in terms of mean and uncertainty (Figures 6a, 6d, 6g). Updating the parameters (scenarios S8 and S13) results in decreased uncertainty during validation (Figures

Hydrol. Earth Syst. Sci. Discuss., https://doi.org/10.5194/hess-2018-18
Manuscript under review for journal Hydrol. Earth Syst. Sci.
Discussion started: 31 January 2018

Hydrology and Earth System Sciences
Open Access
Discussions

6b, 6c, 6e, 6f, 6h, 6i), due to the reduced variability of saturated hydraulic conductivity and van Genuchten parameters. Note also that the update of K_s is particularly beneficial to pressure head (panel a versus b and c) and subsurface outflow (panel g versus h and i) whereas updating α, n, and θ_r improved significantly the water content (panel e versus f).

5.4 Tradeoffs in multi-source data assimilation

We now focus our attention on the scenarios where multi-source data are assimilated. Analogously to the left panels in the same figure, the right panels in Figure 5 show the ratios between $RMSE$ in data assimilation scenarios S7, S10, S15 and the corresponding open loop values for water content, pressure head, and subsurface outflow. Whereas in scenarios S6, S8, and S13 water content alone was assimilated, in scenarios S7, S10, and S15 water content and subsurface outflow were jointly assimilated. The updated variables are system state only in S7, system state and saturated hydraulic conductivity in S10, and system state plus K_s and van Genuchten parameters α, n, and θ_r in S15. As previously noted for the scenarios with assimilation of water content alone, the effect of parameter updating is significant mainly in the validation phase. However, we can now observe an increase in validation $RMSE$ of water content when updating also K_s, with a value that exceeds the one of the corresponding open loop. At the same time, there is a decrease in pressure head $RMSE$ of more than 40% with respect to the open loop, indicating that the update of K_s in this case is beneficial to pressure head, but not to water content. Including the update of van Genuchten parameters, in scenario S15, has an opposite effect: model predictions of water content in validation improve dramatically ($RMSE$ of almost 60% less than in the open loop) while pressure head predictions worsen slightly and align with $RMSE$ values of scenario S13. This indicates that the update of the van Genuchten parameters is more important for predictions of water content than pressure head and represents an interesting example of the kind of the tradeoff associated with multi-source data assimilation and parameter updating in integrated hydrological models.

Further insights about the differences between scenarios S10 and S15 can be gained by looking at Figures 7 and 8, which report the prior and posterior (i.e., at the end of the assimilation period) distributions of soil parameters. Figure 7 reports the results for scenario S10, where K_s only was updated, and shows that the sand K_s is clearly identifiable, whereas the clay K_s is not, with a large residual uncertainty and a mean value that is not consistent with the actual soil type in the hillslope. As no data are available in the clay layer, the large residual variability should be expected, but the bias in the mean value is probably caused by spurious correlations and is likely the reason for the poor model prediction of water content.

Figure 8 shows the prior and posterior distributions of K_s, α, n, and θ_r in S15. Again, for the sand, the saturated hydraulic conductivity can be clearly identified, as well as the exponent n of the van Genuchten retention function, while parameters θ_r and α are more difficult to estimate. As for the clay, posterior uncertainty is large for all the parameters and the mean value of K_s shows again a bias with respect to the prior value, although in this case the final value is more consistent with the actual soil type and this could explain why the water content model predictions improve significantly compared to scenario S10. The results of parameter updating for the clay point out once more that data are needed in all the soil layers and an integrated measurement such as the subsurface outflow is not sufficient to compensate for this lack of representativeness.

Lastly, we analyze the tradeoffs in system state predictions associated to multi-source data assimilation for scenarios S15, S16, and S17. Figure 9 shows pressure head in P2, water content in W6, and subsurface outflow as simulated in the data

assimilation and open loop scenarios, in terms of ensemble mean and 90% confidence bands, compared to the measurements. In scenario S15 (Figures 9a, 9d, 9g), where water content and subsurface discharge were assimilated, model results are very good for these variables but not so for pressure head (see also $NRMSE$ values in Table 4). On the other hand, in scenario S16, where pressure head and subsurface outflow were assimilated, pressure head and discharge are well simulated, but not water content (Figures 9b, 9e, 9h, and Table 4). Finally, in scenario S17, where all the available data were assimilated, the model predicts well both pressure head and water content, but at the cost of a slightly degraded prediction of subsurface outflow compared to scenarios S15 and S16 (Figures 9c, 9f, 9i, and Table 4). This is another example of tradeoff that can be expected in multi-source data assimilation, especially when, for some reasons, not all the different layers or zones of the hillslope or catchment are monitored.

6 Summary and Conclusions

In this study, a Richards equation-based hydrological model, CATHY, has been used with the ensemble Kalman filter to assimilate pressure head, water content, and subsurface outflow data in a real-world test case, represented by an experimental artificial hillslope. A total of 17 data assimilation simulations have been presented and described to provide a comprehensive overview of possible scenarios. Univariate scenarios with the assimilation of water content or pressure head alone were compared to multivariate cases where water content and pressure head were combined with outflow discharge or where water content, pressure head and outflow discharge were jointly assimilated. Regarding the updating strategies, single (state variable) and joint (state variables plus saturated hydraulic conductivity with and without van Genuchten parameters) updating scenarios were considered.

Overall, the capabilities of the ensemble Kalman filter to jointly correct the system states and soil parameters in physically-based hydrological models were confirmed, even in a real-world test case such as the one presented here, characterized by dominant unsaturated dynamics and hence strong nonlinearities. Updating of the saturated hydraulic conductivity brought significant improvements in the prediction of pressure head and subsurface outflow, while updating the van Genuchten parameters proved to be highly beneficial to the prediction of the water content dynamics. On the other hand, multivariate data assimilation may lead to significant tradeoffs. For instance, the assimilation of soil moisture in addition to pressure head and subsurface outflow improved water content, but slightly degraded the prediction of the outflow discharge. Moreover, our results suggest that high-quality and representative data are essential for a proper and effective use of data assimilation in physically-based hydrological models, as shown by the relatively poor performance of the EnKF in scenarios when pressure head was assimilated, due to temperature disturbances of the data, and by biased estimates of clay parameters, due to the lack of data in this soil layer.

In future studies, more representative data, including observations in the clay, will be assimilated and the possibility to apply bias-aware filters will be considered to compensate for the effect of temperature in the tensiometric data.

Acknowledgements. We gratefully acknowledge the financial support of the University of Padova, through the grant CPDA148790.

References

Baatz, D., Kurtz, W., Hendricks Franssen, H.-J., Vereecken, H., and Kollet, S. J.: Catchment tomography - An approach for spatial parameter estimation, Advances in Water Resources, 107, 147 – 159, doi:10.1016/j.advwatres.2017.06.006, 2017.

Bailey, R. and Baù, D.: Ensemble smoother assimilation of hydraulic head and return flow data to estimate hydraulic conductivity distribution, Water Resources Research, 46, W12 543, doi:10.1029/2010WR009147, 2010.

Bertino, L., Evensen, G., and Wackernagel, H.: Sequential Data Assimilation Techniques in Oceanography, International Statistical Review, 71, 223–241, doi:10.1111/j.1751-5823.2003.tb00194.x, 2003.

Bishop, C. H., Etherton, B. J., and Majumdar, S. J.: Adaptive Sampling with the Ensemble Transform Kalman Filter. Part I: Theoretical Aspects, American Meteorological Society, 2001.

Brandhorst, N., Erdal, D., and Neuweiler, I.: Soil moisture prediction with the ensemble Kalman filter: Handling uncertainty of soil hydraulic parameters, Advances in Water Resources, 110, 360 – 370, doi:10.1016/j.advwatres.2017.10.022, 2017.

Cammalleri, C. and Ciraolo, G.: State and parameter update in a coupled energy/hydrologic balance model using ensemble Kalman filtering, Journal of Hydrology, 416-417, 171 – 181, doi:10.1016/j.jhydrol.2011.11.049, 2012.

Camporese, M., Paniconi, C., Putti, M., and Salandin, P.: Ensemble Kalman filter data assimilation for a process-based catchment scale model of surface and subsurface flow, Water Resources Research, 45, W10 421, doi:10.1029/2008WR007031, 2009a.

Camporese, M., Paniconi, C., Putti, M., and Salandin, P.: Comparison of Data Assimilation Techniques for a Coupled Model of Surface and Subsurface Flow, Vadose Zone J., 2009b.

Camporese, M., Paniconi, C., Putti, M., and Orlandini, S.: Surface-subsurface flow modeling with path-based runoff routing, boundary condition-based coupling, and assimilation of multisource observation data, Water Resources Research, 46, W02 512, doi:10.1029/2008WR007536, 2010.

Carsel, R. F. and Parrish, R. S.: Developing joint probability distributions of soil water retention characteristics, Water Resources Research, 24, 755–769, doi:10.1029/WR024i005p00755, 1988.

Chen, Y. and Zhang, D.: Data assimilation for transient flow in geologic formations via ensemble Kalman filter, Advances in Water Resources, 29, 1107 – 1122, doi:10.1016/j.advwatres.2005.09.007, 2006.

Clark, M. P., Rupp, D. E., Woods, R. A., Zheng, X., Ibbitt, R. P., Slater, A. G., Schmidt, J., and Uddstrom, M. J.: Hydrological data assimilation with the ensemble Kalman filter: Use of streamflow observations to update states in a distributed hydrological model, Advances in Water Resources, 31, 1309 – 1324, doi:10.1016/j.advwatres.2008.06.005, 2008.

Crow, W. T. and Wood, E. F.: The assimilation of remotely sensed soil brightness temperature imagery into a land surface model using Ensemble Kalman filtering: a case study based on ESTAR measurements during SGP97, Advances in Water Resources, 26, 137 – 149, doi:10.1016/S0309-1708(02)00088-X, 2003.

De Lannoy, G. J., Houser, P. R., Pauwels, V., and Verhoest, N. E.: State and bias estimation for soil moisture profiles by an ensemble Kalman filter: Effect of assimilation depth and frequency, Water Resources Research, 2007.

Erdal, D., Neuweiler, I., and Wollschläger, U.: Using a bias aware EnKF to account for unresolved structure in an unsaturated zone model, Water Resources Research, 50, 132–147, doi:10.1002/2012WR013443, 2014.

Erdal, D., Rahman, M., and Neuweiler, I.: The importance of state transformations when using the ensemble Kalman filter for unsaturated flow modeling: Dealing with strong nonlinearities, Advances in Water Resources, 86, 354 – 365, doi:10.1016/j.advwatres.2015.09.008, 2015.

Evensen, G.: The Ensemble Kalman Filter: theoretical formulation and practical implementation, Ocean Dynamics, 53, 2003.

Evensen, G.: Data Assimilation, Springer, 2009a.

Evensen, G.: The ensemble Kalman filter for combined state and parameter estimation, vol. 29, IEEE Control Systems, 2009b.

Flores, A. N., Bras, R. L., and Entekhabi, D.: Hydrologic data assimilation with a hillslope-scale-resolving model and L band radar observations: Synthetic experiments with the ensemble Kalman filter, Water Resources Research, 2012.

Francois, C., Quesney, A., and Ottlé, C.: Sequential Assimilation of ERS-1 SAR Data into a Coupled Land Surface–Hydrological Model Using an Extended Kalman Filter, Journal of Hydrometeorology, 4, 2003.

Hain, C. R., Crow, W. T., Anderson, M. C., and Mecikalski, J. R.: An ensemble Kalman filter dual assimilation of thermal infrared and microwave satellite observations of soil moisture into the Noah land surface model, Water Resources Research, 2012.

Han, X. and Li, X.: An evaluation of the nonlinear/non-Gaussian filters for the sequential data assimilation, Remote Sensing of Environment, 2008.

Hendricks Franssen, H.-J. and Kinzelbach, W.: Real-time groundwater flow modeling with the Ensemble Kalman Filter: Joint estimation of states and parameters and the filter inbreeding problem, Water Resources Research, 44, W09 408, doi:10.1029/2007WR006505, 2008.

Johnson, S. K.: Distributions in Statistics: Continuous Unvariate Distributions-1, Houghton Mifflin, 1970.

Kollet, S., Sulis, M., Maxwell, R. M., Paniconi, C., Putti, M., Bertoldi, G., Coon, E. T., Cordano, E., Endrizzi, S., Kikinzon, E., Mouche, E., Mügler, C., Park, Y.-J., Refsgaard, J. C., Stisen, S., and Sudicky, E.: The integrated hydrologic model intercomparison project, IH-MIP2: A second set of benchmark results to diagnose integrated hydrology and feedbacks, Water Resources Research, 53, 867–890, doi:10.1002/2016WR019191, 2017.

Kurtz, W., He, G., Kollet, S., Maxwell, R., Vereecken, H., and Hendricks Franssen, H.-J.: TerrSysMP-PDAF (version 1.0): A modular high-performance data assimilation framework for an integrated land surface-subsurface model, Geoscientific Model Development, 2016.

Li, L., Zhou, H., Gómez-Hernández, J. J., and Hendricks Franssen, H.-J.: Jointly mapping hydraulic conductivity and porosity by assimilating concentration data via ensemble Kalman filter, Journal of Hydrology, 2012.

Lora, M., Camporese, M., and Salandin, P.: Design and performance of a nozzle-type rainfall simulator for landslide triggering experiments, CATENA, 140, 77 – 89, doi:10.1016/j.catena.2016.01.018, 2016.

Maxwell, R. M., Putti, M., Meyerhoff, S., Delfs, J.-O., Ferguson, I. M., Ivanov, V., Kim, J., Kolditz, O., Kollet, S. J., Kumar, M., Lopez, S., Niu, J., Paniconi, C., Park, Y.-J., Phanikumar, M. S., Shen, C., Sudicky, E. A., and Sulis, M.: Surface-subsurface model intercomparison: A first set of benchmark results to diagnose integrated hydrology and feedbacks, Water Resources Research, 50, 1531–1549, doi:10.1002/2013WR013725, 2014.

Monsivais-Huertero, A., Graham, W. D., Judge, J., and Agrawal, D.: Effect of simultaneous state-parameter estimation and forcing uncertainties on root-zone soil moisture for dynamic vegetation using EnKF, Advances in Water Resources, 33, 468 – 484, doi:10.1016/j.advwatres.2010.01.011, 2010.

Montzka, C., Pauwels, V. R. N., Hendricks Franssen, H.-J., Han, X., and Vereecken, H.: Multivariate and Multiscale Data Assimilation in Terrestrial Systems: A Review, Sensors, 12, 16 291–16 333, doi:10.3390/s121216291, 2012.

Moradkhani, H.: Hydrologic remote sensing and land surface data assimilation, Sensors, 2008.

Moradkhani, H., Hsu, K.-L., Gupta, H., and Sorooshian, S.: Uncertainty assessment of hydrologic model states and parameters: Sequential data assimilation using the particle filter, Water resources research, 2005.

Pan, M. and Wood, E. F.: Data Assimilation for Estimating the Terrestrial Water Budget Using a Constrained Ensemble Kalman Filter, Journal of Hydrometeorology, 7, 534–547, doi:10.1175/JHM495.1, 2006.

Pasetto, D., Camporese, M., and Putti, M.: Ensemble Kalman filter versus particle filter for a physically-based coupled surface–subsurface model, Advances in water resources, 2012.

Pasetto, D., Niu, G.-Y., Pangle, L., Paniconi, C., Putti, M., and Troch, P. A.: Impact of sensor failure on the observability of flow dynamics at the Biosphere 2 LEO hillslopes, Advances in Water Resources, 86, 327 – 339, doi:10.1016/j.advwatres.2015.04.014, 2015.

Rasmussen, J., Madsen, H., Jensen, K. H., and Refsgaard, J. C.: Data assimilation in integrated hydrological modelling in the presence of observation bias, Hydrology and Earth System Sciences Discussions, 12, 2015a.

Rasmussen, J., Madsen, H., Jensen, K. H., and Refsgaard, J. C.: Data assimilation in integrated hydrological modeling using ensemble Kalman filtering: evaluating the effect of ensemble size and localization on filter performance, Hydrol. Earth Syst. Sci., 19, 2015b.

Reichle, R. H., McLaughlin, D. B., and Entekhabi, D.: Hydrologic data assimilation with the ensemble Kalman filter, Monthly Weather Review, 130, 2002a.

Reichle, R. H., Walker, J. P., Koster, R. D., and Houser, P. R.: Extended versus ensemble Kalman filtering for land data assimilation, Journal of hydrometeorology, 3, 2002b.

Ridler, M.-E., Madsen, H., Stisen, S., Bircher, S., and Fensholt, R.: Assimilation of SMOS-derived soil moisture in a fully integrated hydrological and soil-vegetation-atmosphere transfer model in Western Denmark, Water Resources Research, 50, 8962–8981, doi:10.1002/2014WR015392, 2014.

Sakov, P., Evensen, G., and Bertino, L.: Asynchronous data assimilation with the EnKF, Tellus A, 62, 24–29, doi:10.1111/j.1600-0870.2009.00417.x, 2010.

Schenato, L., Palmieri, L., Camporese, M., Bersan, S., Cola, S., Pasuto, A., Galtarossa, A., Salandin, P., and Simonini, P.: Distributed optical fibre sensing for early detection of shallow landslides triggering, Scientific Reports, 7, 14 686, doi:10.1038/s41598-017-12610-1, 2017.

Shi, Y., Davis, K. J., Zhang, F., Duffy, C. J., and Yu, X.: Parameter estimation of a physically-based land surface hydrologic model using an ensemble Kalman filter: A multivariate real-data experiment, Advances in Water Resources, 83, 421 – 427, doi:10.1016/j.advwatres.2015.06.009, 2015.

Tang, Q., Kurtz, W., Schilling, O. S., Brunner, P., Vereecken, H., and Hendricks Franssen, H.-J.: The influence of riverbed heterogeneity patterns on river-aquifer exchange fluxes under different connection regimes, Journal of Hydrology, 554, 383 – 396, doi:10.1016/j.jhydrol.2017.09.031, 2017.

Troch, P. A., Paniconi, C., and McLaughlin, D.: Catchment-scale hydrological modeling and data assimilation, Advances in Water Resources, 26, 131 – 135, doi:10.1016/S0309-1708(02)00087-8, 2003.

van Genuchten, M. T.: A closed-form equation for predicting the hydraulic conductivity of unsaturated soils, Soil Science Society of America Journal, 44, 892–898, doi:10.2136/sssaj1980.03615995004400050002x, 1980.

Visser, A., Stuurman, R., and Bierkens, M. F.: Real-time forecasting of water table depth and soil moisture profiles, Advances in Water Resources, 2006.

Vrugt, J. A., Gupta, H. V., Nualláin, B., and Bouten, W.: Real-Time Data Assimilation for Operational Ensemble Streamflow Forecasting, Journal of Hydrometeorology, 7, 548–565, doi:10.1175/JHM504.1, 2006.

Warrick, A. W., Wierenga, P. J., Young, M. H., and Musil, S. A.: Diurnal fluctuations of tensiometric readings due to surface temperature changes, Water Resources Research, 34, 2863–2869, doi:10.1029/98WR02095, 1998.

Weerts, A. H. and El Serafy, G. Y.: Particle filtering and ensemble Kalman filtering for state updating with hydrological conceptual rainfall-runoff models, Water Resources Research, 2006.

Hydrol. Earth Syst. Sci. Discuss., https://doi.org/10.5194/hess-2018-18
Manuscript under review for journal Hydrol. Earth Syst. Sci.
Discussion started: 31 January 2018

Hydrology and Earth System Sciences
Discussions

Table 1. Perturbation parameters for the generation of the ensemble initial conditions, hydraulic conductivities and atmospheric forcing.

Variable	Units	Nominal value(s)	Perturbation type	Mean	Standard deviation
ψ_0	m	-0.67	additive	0	0.2
Atmospheric forcing[a]	mm/h	58.8; 47.5; -0.0284	multiplicative	1	0.2
		Sand			
K_s	m/s	10^{-4}	multiplicative	1.17	1.53
S_s	m^{-1}	10^{-3}	not perturbed		
ϕ	-	0.58	not perturbed		
θ_r	-	0.065	see Section 4.2		0.25[b]
α	cm^{-1}	0.070	see Section 4.2		0.25[b]
n	-	1.88	see Section 4.2		0.25[b]
		Clay			
K_s	m/s	10^{-7}	multiplicative	1.17	1.53
S_s	m^{-1}	5×10^{-3}	not perturbed		
ϕ	-	0.40	not perturbed		
θ_r	-	0.067	see Section 4.2		0.25[b]
α	cm^{-1}	0.017	see Section 4.2		0.25[b]
n	-	1.40	see Section 4.2		0.25[b]

[a] Rainfall (positive) and evaporation (negative) rates.

[b] σ_{VG} as described in Section 4.2.

Xie, X. and Zhang, D.: Data assimilation for distributed hydrological catchment modeling via ensemble Kalman filter, Advances in Water Resources, 33, 678 – 690, doi:10.1016/j.advwatres.2010.03.012, 2010.

Zhang, D., Madsen, H., Ridler, M. E., Refsgaard, J. C., and Jensen, K. H.: Impact of uncertainty description on assimilating hydraulic head in the MIKE SHE distributed hydrological model, Advances in Water Resources, 86, 400–413, doi:10.1016/j.advwatres.2015.07.018, 2015.

Zhang, D., Madsen, H., Ridler, M. E., Kidmose, J., and Jensen, K. H.: Multivariate hydrological data assimilation of soil moisture and groundwater head, Hydrology and Earth System Sciences, 20, 2016.

Zhang, H., Kurtz, W., Kollet, S., Vereecken, H., and Hendricks Franssen, H.-J.: Comparison of different assimilation methodologies of groundwater levels to improve predictions of root zone soil moisture with an integrated terrestrial system model, Advances in Water Resources, 111, 224 – 238, doi:10.1016/j.advwatres.2017.11.003, 2018.

Zovi, F., Camporese, M., Hendricks Franssen, H.-J., Huisman, J. A., and Salandin, P.: Identification of high-permeability subsurface structures with multiple point geostatistics and normal score ensemble Kalman filter, Journal of Hydrology, 548, 208 – 224, doi:10.1016/j.jhydrol.2017.02.056, 2017.

Hydrol. Earth Syst. Sci. Discuss., https://doi.org/10.5194/hess-2018-18
Manuscript under review for journal Hydrol. Earth Syst. Sci.
Discussion started: 31 January 2018

Hydrology and Earth System Sciences
Discussions

Table 2. Factored covariance matrices used for the perturbation of van Genuchten parameters (from Carsel and Parrish, 1988)).

		θ_r	α	n
Sandy loam	θ_r	0.538	0.017	-0.194
	α		0.014	0.019
	n			0.108
Silt loam	θ_r	0.522	0.030	-0.17
	α		0.082	0.234
	n			0.158

Table 3. Overview of the open loop and data assimilation scenarios.

Scenario[1]	Assimilation interval	Assimilated variables[2]	Updated variables[3]	σ_{VG}
OL1	-	-	-	0.1
OL2	-	-	-	0.25
S1	3 h	WC	St. var., K_s	0.1
S2	3 h	PH	St. var., K_s	0.1
S3	3 h	WC, Q	St. var., K_s	0.1
S4	3 h	PH, Q	St. var., K_s	0.1
S5	3 h	WC, PH, Q	St. var., K_s	0.1
S6	1 h	WC	St. var.	0.1
S7	1 h	WC, Q	St. var.	0.1
S8	1 h	WC	St. var., K_s	0.1
S9	1 h	PH	St. var., K_s	0.1
S10	1 h	WC, Q	St. var., K_s	0.1
S11	1 h	PH, Q	St. var., K_s	0.1
S12	1 h	WC, PH, Q	St. var., K_s	0.1
S13	1 h	WC	St. var., K_s, V.G.	0.25
S14	1 h	PH	St. var., K_s, V.G.	0.25
S15	1 h	WC, Q	St. var., K_s, V.G.	0.25
S16	1 h	PH, Q	St. var., K_s, V.G.	0.25
S17	1 h	WC, PH, Q	St. var., K_s, V.G.	0.25

[1] OL1 and OL2 indicate open loop scenarios, i.e., simulations without data assimilation.

[2] WC, PH, and Q denote water content, pressure head, and subsurface outflow, respectively.

[3] St. var., K_s, and V.G. indicate state variables (in terms of pressure head), saturated hydraulic conductivity, and van Genuchten parameters, respectively.

Hydrol. Earth Syst. Sci. Discuss., https://doi.org/10.5194/hess-2018-18
Manuscript under review for journal Hydrol. Earth Syst. Sci.
Discussion started: 31 January 2018

Hydrology and Earth System Sciences
Discussions

Table 4. Normalized root mean square errors ($NRMSE$) for the 17 data assimilation scenarios under analysis and two open loop (OL) simulations. The table reports the $NRMSE$ for three variables, water content, pressure head and outflow discharge, both for the assimilation and the validation periods. The last three columns report the mean values calculated over the three variables (WC, PH and Q) and the global average between assimilation and validation. Bold values indicate exceedance of the corresponding open loop errors.

	$NRMSE_{WC}$		$NRMSE_{PH}$		$NRMSE_{Q}$		Mean $NRMSE$		
Scenario	Assimilation	Validation	Assimilation	Validation	Assimilation	Validation	Assimilation	Validation	Global
OL1	0.16	0.14	0.45	0.36	0.72	0.64	0.44	0.38	0.41
OL2	0.16	0.13	0.46	0.36	0.71	0.63	0.44	0.38	0.41
S1	0.09	0.11	0.33	0.27	0.58	0.53	0.33	0.30	0.32
S2	**0.21**	**0.24**	0.21	0.31	0.51	0.47	0.31	0.34	0.33
S3	0.10	**0.16**	0.31	0.21	0.63	0.56	0.34	0.31	0.33
S4	**0.24**	**0.26**	0.25	**0.39**	**0.82**	**0.73**	0.44	**0.46**	**0.45**
S5	**0.18**	**0.22**	0.23	0.26	0.70	0.64	0.37	0.37	0.37
S6	0.07	0.12	0.36	0.36	0.68	0.62	0.37	0.37	0.37
S7	0.08	0.12	0.33	0.33	0.55	0.50	0.32	0.31	0.32
S8	0.08	0.11	0.32	0.27	0.55	0.49	0.32	0.29	0.30
S9	**0.22**	**0.24**	0.17	0.29	0.46	0.42	0.29	0.32	0.30
S10	0.09	**0.18**	0.31	0.21	0.54	0.48	0.31	0.29	0.30
S11	**0.24**	**0.33**	0.22	**0.83**	0.59	0.54	0.35	**0.57**	**0.46**
S12	**0.19**	**0.31**	0.20	**0.68**	0.62	0.55	0.34	**0.51**	**0.43**
S13	0.07	0.06	0.32	0.28	0.52	0.49	0.30	0.28	0.29
S14	**0.33**	**0.41**	0.16	0.21	0.50	0.45	0.33	0.36	0.34
S15	0.07	0.05	0.31	0.29	0.53	0.51	0.31	0.28	0.29
S16	**0.42**	**0.48**	0.18	0.19	0.60	0.57	0.40	**0.41**	0.41
S17	0.10	0.05	0.22	0.29	0.69	**0.66**	0.34	0.34	0.34

Hydrol. Earth Syst. Sci. Discuss., https://doi.org/10.5194/hess-2018-18
Manuscript under review for journal Hydrol. Earth Syst. Sci.
Discussion started: 31 January 2018

Hydrology and Earth System Sciences
Discussions
Open Access
EGU

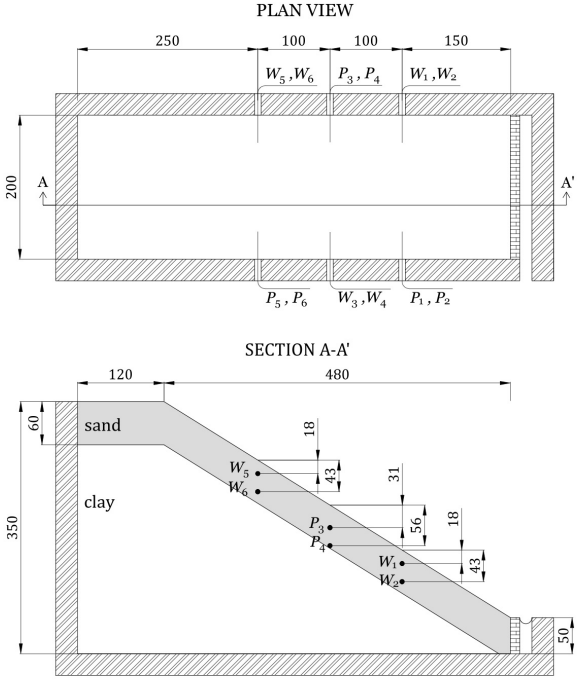

Figure 1. Plan view and longitudinal cross-section of the artificial hillslope, along with the position of the monitoring instruments. Tensiometers are indicated by the letter "P", while WCR probes are denoted by "W". All dimensions are in cm.

Hydrol. Earth Syst. Sci. Discuss., https://doi.org/10.5194/hess-2018-18
Manuscript under review for journal Hydrol. Earth Syst. Sci.
Discussion started: 31 January 2018

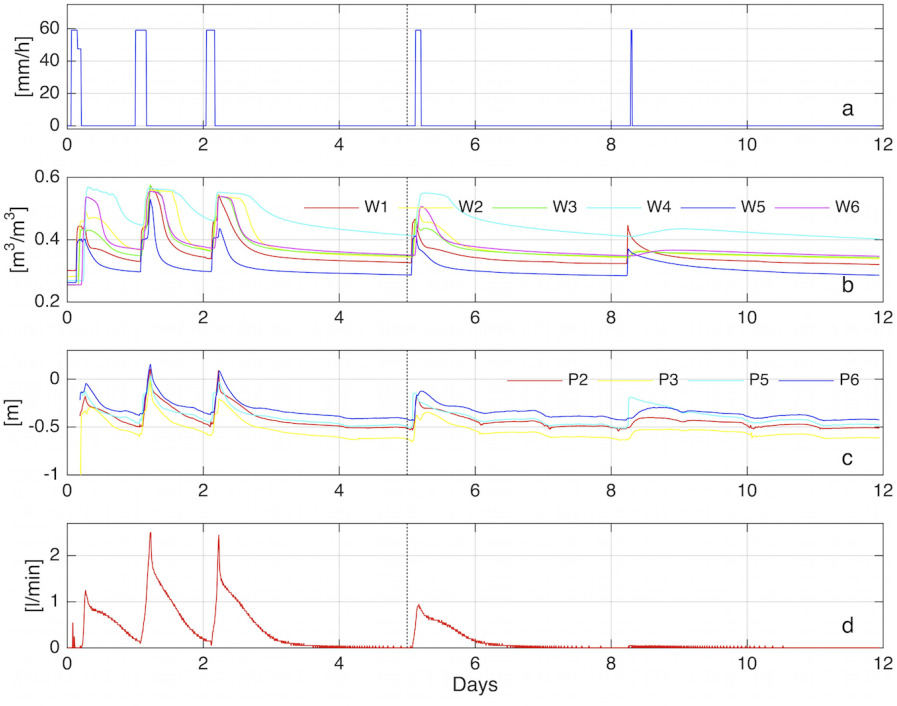

Figure 2. Experimental data collected during the experiment: a) rainfall rate; b) water content as measured by the WCR probes; c) pressure head as measured by the tensiometers; d) subsurface outflow. The black vertical dashed line marks the transition between the data assimilation and the validation phases.

Hydrol. Earth Syst. Sci. Discuss., https://doi.org/10.5194/hess-2018-18
Manuscript under review for journal Hydrol. Earth Syst. Sci.
Discussion started: 31 January 2018

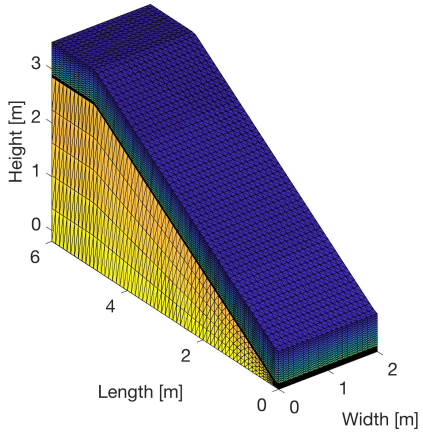

Figure 3. Three-dimensional finite element grid of the hillslope.

Hydrol. Earth Syst. Sci. Discuss., https://doi.org/10.5194/hess-2018-18
Manuscript under review for journal Hydrol. Earth Syst. Sci.
Discussion started: 31 January 2018

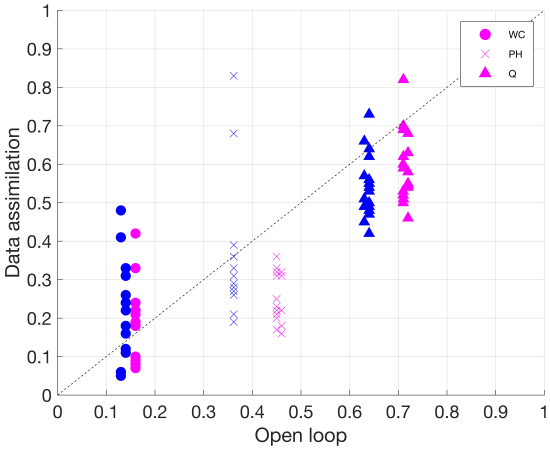

Figure 4. Normalized root mean square errors for water content, pressure head, and subsurface outflow of the data assimilation scenarios versus corresponding values of the open loop. Symbols in magenta represent values calculated over the assimilation period, while symbols in blue represent values calculated over the validation period.

Hydrol. Earth Syst. Sci. Discuss., https://doi.org/10.5194/hess-2018-18
Manuscript under review for journal Hydrol. Earth Syst. Sci.
Discussion started: 31 January 2018

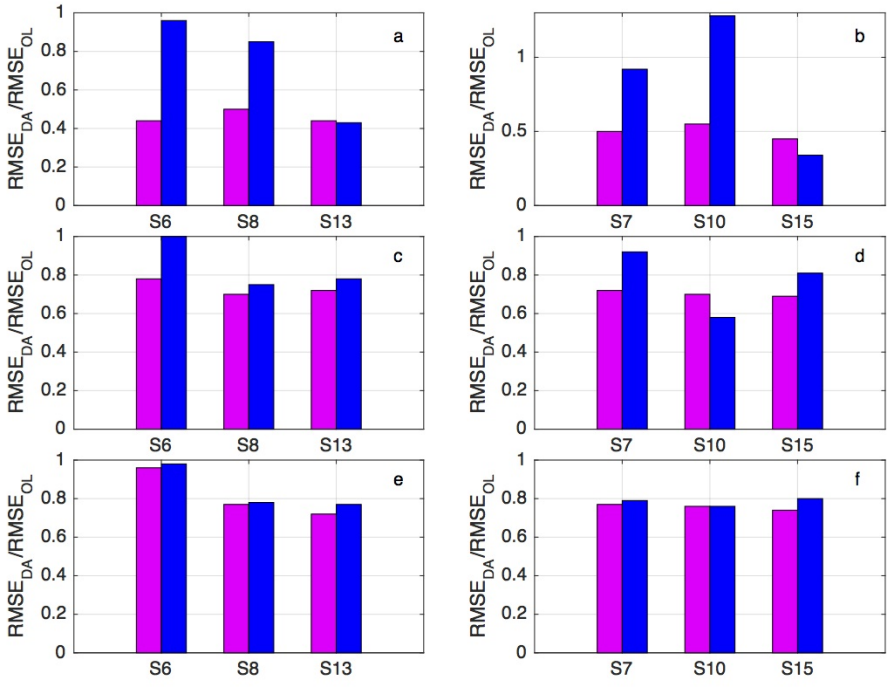

Figure 5. Ratios between $RMSE$s in scenarios S6, S8, S13 (panels a, c, e), and S7, S10, S15 (panels b, d, f) and the corresponding open loop values, for water content, WC (a and b), pressure head, PH (c and d), and subsurface outflow, Q (e and f). The magenta bars refer to the data assimilation period, while the blue ones to the validation period.

Hydrol. Earth Syst. Sci. Discuss., https://doi.org/10.5194/hess-2018-18
Manuscript under review for journal Hydrol. Earth Syst. Sci.
Discussion started: 31 January 2018

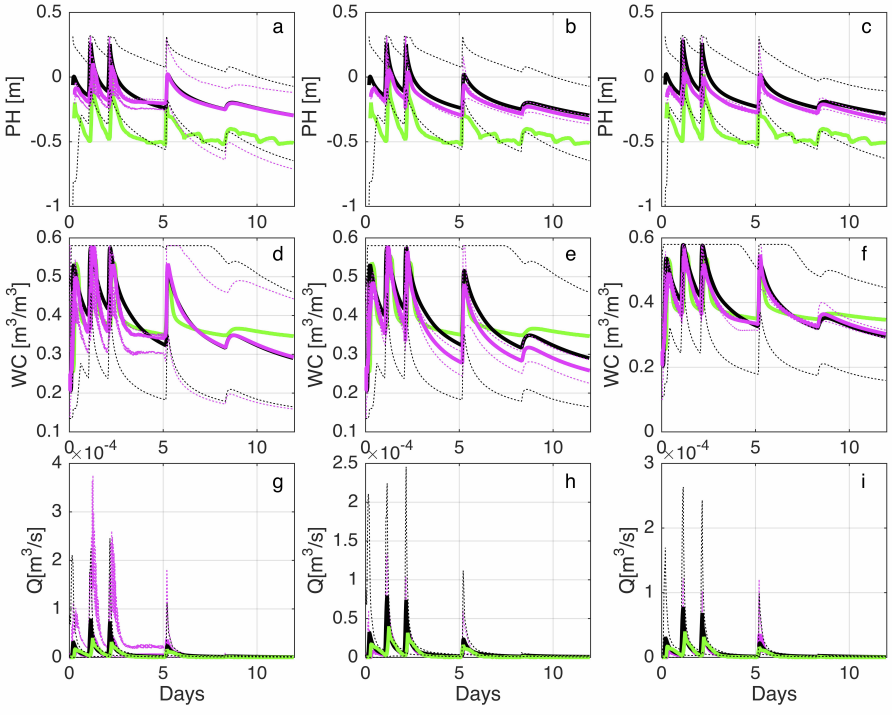

Figure 6. Plots of the pressure head in P2, (a, b and c), water content in W6, (d, e, f) and outflow discharge (g, h, i) for scenarios S6 (a, d, g), S8 (b, e, h), and S13 (c, f, i). Solid green lines represent experimental data while solid black and magenta lines indicate the ensemble mean of the open loop and data assimilation scenarios, respectively. The simulated 90% confidence bands are also reported (dashed black and magenta lines). The locations of the tensiometer P2 and water content probe W6 are shown in Figure 1.

Hydrol. Earth Syst. Sci. Discuss., https://doi.org/10.5194/hess-2018-18
Manuscript under review for journal Hydrol. Earth Syst. Sci.
Discussion started: 31 January 2018

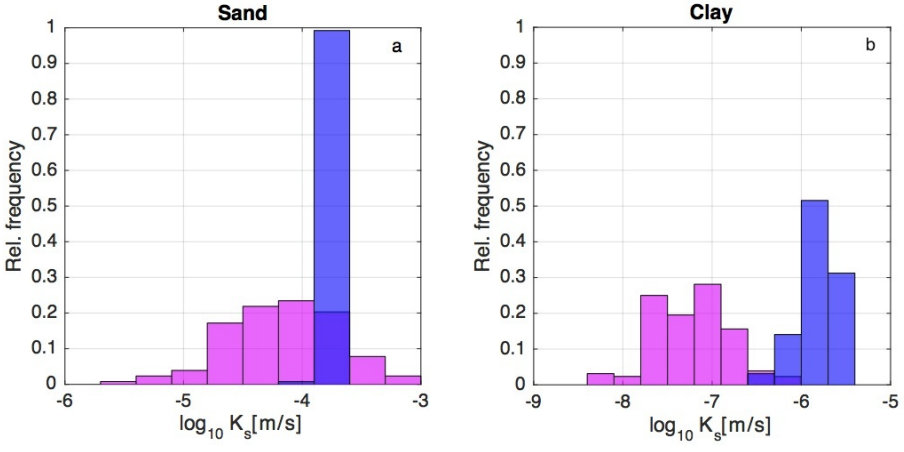

Figure 7. Relative frequency distributions of the saturated hydraulic conductivity, K_s, of sand and clay in scenario S10. Graphs in magenta denote the prior K_s distributions, while the blue ones indicate the posterior distributions, i.e., at the end of the assimilation period.

Hydrol. Earth Syst. Sci. Discuss., https://doi.org/10.5194/hess-2018-18
Manuscript under review for journal Hydrol. Earth Syst. Sci.
Discussion started: 31 January 2018

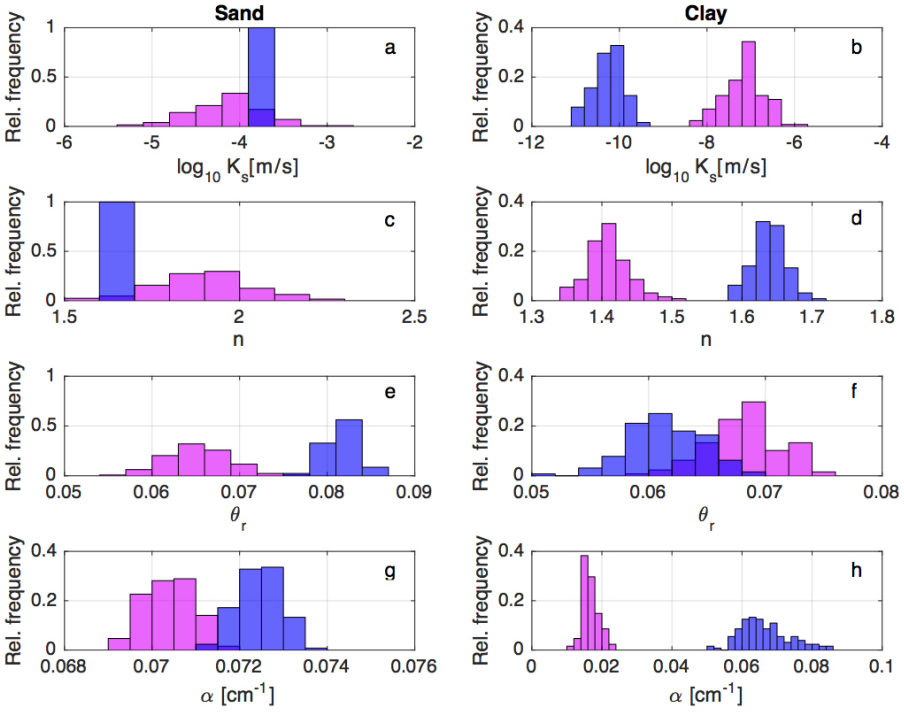

Figure 8. Relative frequency distributions of the saturated hydraulic conductivity, K_s, and van Genucthen parameters of sand and clay in scenario S15. Graphs in magenta denote prior distributions, while the blue ones indicate posterior distributions, i.e., at the end of the assimilation period.

Hydrol. Earth Syst. Sci. Discuss., https://doi.org/10.5194/hess-2018-18
Manuscript under review for journal Hydrol. Earth Syst. Sci.
Discussion started: 31 January 2018

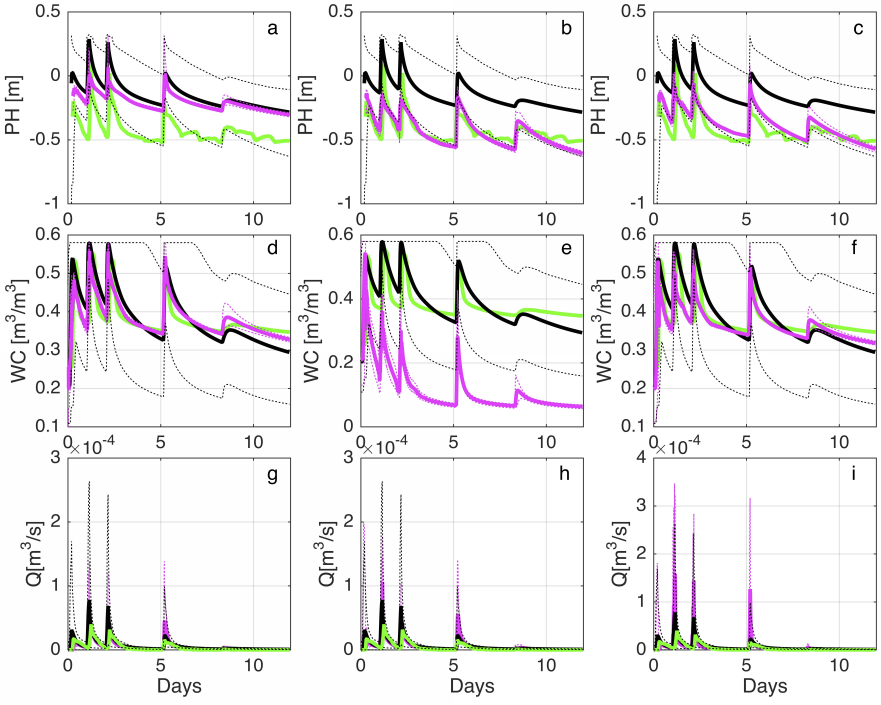

Figure 9. Plots of the pressure head in P2, (a, b and c), water content in W6, (d, e, f) and outflow discharge (g, h, i) for scenarios S15 (a, d, g), S16 (b, e, h), and S17 (c, f, i). Solid green lines represent experimental data while solid black and magenta lines indicate the ensemble mean of the open loop and data assimilation scenarios, respectively. The simulated 90% confidence bands are also reported (dashed black and magenta lines). The locations of the tensiometer P2 and water content probe W6 are shown in Figure 1.